ORIGINAL ARTICLE

Linearly polarized IR-spectroscopy of partially oriented solids as a colloid suspension in nematic host: a tool for spectroscopic and structural elucidation of the embedded chemicals

B. B. Koleva · T. M. Kolev · V. Simeonov · T. Spassov · M. Spiteller

Abstract Colloid suspensions *in nematic liquid crystal* were employed for the first time in 2004 as a tool for the partial orientation of solids, to be examined by linearly polarized IR-(IR-LD) spectroscopy. It has been found is found that a partial orientation (15–20%) of suspended particles, is adequate for the recording of reasonable linearly polarized IR-spectra is achieved when: $5 \pm 1\%$ by weight of the given solid compound (*organic, inorganic, transition metal complex or glass*) with particle size within the limits 0.3–0.9 μm is mixed with a nematic liquid crystal substance (ZLI 1695, ZLI 1538 or MLC 6815) suitable for IR spectroscopy and the slightly viscous suspension obtained is phase pressed between two KBr-plates. These latter are roughened in one direction prior to use with fine sandpaper (C800) (size 5 μm). Then, the KBr-plattes and pressed suspension are moved repeatedly with 3 μm/s for 100 times. The optimal cell thickness is 100 μm. If mathematical procedures are used for polarized IR-spectra interpretation, then it is possible to perform structural elucidation of the embedded compounds, independently of their melting point, crystalline or amorphous state, and the quality of the monocrystals or polycrystalline of the e sample. The method permits the study of organic and inorganic compounds, transition metal complexes and glasses. Here we will discuss the fundamental questions concerning the above state such as the morphology of the suspended particles, the particle size, the influence of the physical chemistry properties of liquid crystal medium on the degree of orientation of suspended particles; the velocity of the shearing of the suspension, the degree of the roughening of the KBr-plates and their effects on the degree of orientation, the influence of the space group on the orientation parameter, the nature and balance of the forces acting on the suspended particles; their degree of orientation, the mathematical model used. Conventional and linearly polarized IR-spectroscopy and electron microscopy are used for elucidation of these points. Statistical approaches have also been applied in order to estimate the impact of the experimental parameters (size, velocity, thickness) on the IR-signal for each of the 13 systems studied. An experimental design of the type involving full factorial design on two levels of variation of the input factors is presented.

B. B. Koleva (✉)
Faculty of Chemistry, Ruhr-University Bochum, 4478 Bochum, Germany
e-mail: BKoleva@chem.uni-sofia.bg

T. M. Kolev · M. Spiteller
Institute of Environmental Research, University of Dortmund, 44221 Dortmund, Germany

V. Simeonov
Faculty of Chemistry, Department of Analytical Chemistry, University of Sofia "St. Kl. Ohridsky", Sofia 1164, Bulgaria

T. Spassov
Faculty of Chemistry, Department of Applied Inorganic Chemistry, University of Sofia "St. Kl. Ohridsky", Sofia 1164, Bulgaria

Introduction

Colloidal suspensions in nematic liquid crystals have been intensively studied, on account of their attracting wide

interest for application in telecommunications, the Hi Tech, industry, medicine and fundamental research [1–7]. They have been described as new attractive soft matter systems since new interesting phenomena arise through the combination of colloidal suspensions and liquid crystals [3, 4, 8–13]. They were developed and applied as a new tool for orientation of solids and applied in linearly polarized infrared (IR-LD) spectroscopy for IR-band assignment and structural elucidation in 2004 for first time using a model organic complex system by Ivanova et al. [14]. Before that time, only three orientation techniques of solids had been described: (i) polymer orientation by stretching; single crystal growing followed by direct IR-LD measurements and polycrystalline sample oriented after melting the solid compounds between in previously roughened KBr plates [15–21]. However, difficult technical problems are involved in these techniques, for example growing a "good quality" monocrystalline sample or the temperature of 170 °C involved in the melting technique, which is a critical value for KBr plates. The orientation method involving a colloidal suspension in a nematic liquid crystal gets around many of these problems. It is readily carried out; the samples are prepared as suspensions at room temperature. The technique is fast, cheap and easy to employ. The orientation does not depend on the melting point of the compound under investigation, the quality of the monocrystalline or the polycrystalline sample. Its advantage lies not only in the possibility of experimental IR-band assignment of suspended compounds but on the possibility of obtaining of structural or local structural information in solids, where the application of the single crystal X-ray diffraction method is impossible as for example with amorphous compounds and glasses. The idea of obtaining the structural information by means of IR-LD spectroscopy is has been reported [18, 19], where the determination of α- and β-helices has been demonstrated on oriented polymers [18, 19]. However, the structural and local structural information for amorphous samples and glasses has been only been obtained in the papers presented here for more then 80 organic compounds, their transition metal complexes, 7 inorganic models and 6 tellurite and borate glasses. Details have been given [22–29]. The validation of the orientation tool for accuracy, precision and the influence of the host on peak positions and integral absorbances of guest molecule bands; the optimization of some experimental conditions (number of scans, the roughening of the KBr-pellets, the quantity of compound studied to be included in the liquid crystal medium, the ratios of Lorentzian to Gaussian peak functions in the curve fitting procedure on the spectroscopic signal at five different frequencies and an experimental design for quantitative evaluation of the impact of four input factors have already been reported [30, 31]. However, until now

there has been no discussion of in any of these investigations concerning the fundamental questions of this orientation tool, i.e. about the morphology of the suspended particles, particle size, influence of the physical chemical properties of liquid crystal medium on the degree of orientation of suspended particles; the velocity of the shearing of the suspension, the degree of roughening of the KB-plates and its effect on the degree of orientation, the influence of the space group on the orientation parameter of the compound studied, the nature and balance of the forces acting on the suspended particles; their degree of orientation, the mathematical model and etc. In this paper we present a systematic study dealing with these latter problems using the possibilities of IR-LD spectroscopy of oriented solid samples as a colloidal suspension in nematic liquid crystal, electron spectroscopy and chemometry, as applied to 13 organic model systems oriented in 3 different, nematic liquid crystal hosts suitable for IR-LD measurements.

Experimental

Materials and methods

IR-spectroscopic measurements within 4000–400 cm^{-1} range were obtained on a Thermo Nicolet OMNIC NEXUS FT-IR spectrometer (resolution of 0.5 cm^{-1} and 250 scans). A Specac wire-grid polarizer was used for recording polarized IR-spectra.

Oriented solid samples were obtained by *colloid suspension in a nematic liquid crystal* using three mesomorphic media: ZLI 1695, Merck, MLC 6815 and ZLI 1538 (Merck, Germany). The selection of the orientation medium, i.e. the nematic liquid crystal, is based on the fact that, their self-absorbtion in the middle IR-spectroscopic region must be minimal. 4-Cyano-4′-bicycloxehyl liquid crystals a suitable host media for orientation, since its weak IR-spectrum permits, recording of the guest-compound IR-bands in the whole 4000–400 cm^{-1} range (Fig. 1). Apart from the regions 2800–3000 cm^{-1}, near 2235 cm^{-1}, 1457 cm^{-1} and 896 cm^{-1} in ZLI 1695 (Fig. 1(1)) and MLC 1538 (Fig. 1(3)), rest of the region is available. In the case of MLC 6815, the presence of the ester groups narrow the IR-spectroscopic range possible for analysis obliterating the regions about 1723 cm^{-1} and within 1447–896 cm^{-1} (Fig. 1(2)). A mesomorphic interval including room temperature is another important characteristic for an orientation medium. ZLI 1695 and MLC 6815 a mesomorphic interval that includes 25 °C. However the S–N transition temperature of ZLI 1538 is 54 °C, so that the suspension must be prepared and recoded in a thermostat. Other advantages of the of liquid crystals selected are their physical-chemistry properties (ZLI 1695: clearing point of

Fig. 1 IR-spectra of the liquid crystals ZLI 1695 (1), MLC 6815 (2) and ZLI 1538 (3)
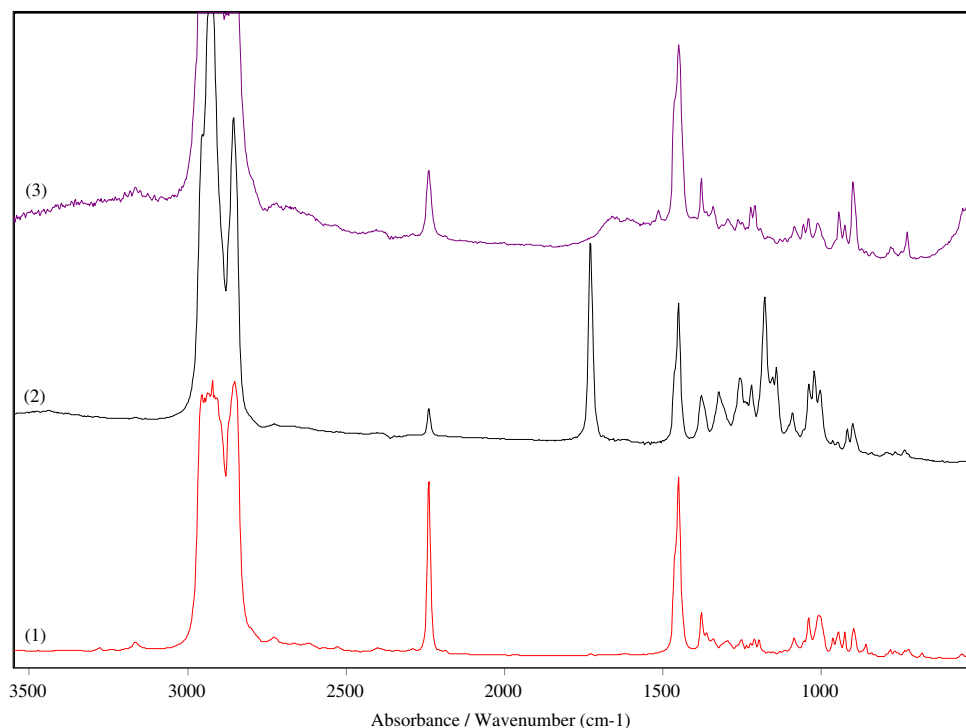
72 °C, viscosity 62 mm^2/s at 20 °C, dielectric anisotropy 4.2 at 20 °C and 1 kHz, optical anisotropy 0.0600 at 20 °C and 589 nm; MLC 6815: clearing point of 67 °C, dielectric anisotropy 8.1 at 20 °C and 1 kHz, optical anisotropy 0.0517 at 20 °C and 589 nm; ZLI 1538: clearing point of 79 °C, viscosity 68 mm^2/s at 20 °C, dielectric anisotropy 3.8 at 20 °C and 1 kHz, optical anisotropy 0.0500 at 20 °C and 589 nm;) so that it is possible to orientate polar solid compounds in ZLI 1695 and ZLI 1538 and non-polar compounds in MLC 6815. The isolated nitrile stretching IR-band at about 2235 cm^{-1} serves in addition as an orientation indicator.

The effective orientation of the samples was achieved by mixing 5 ± 1% by weight of the compound to be studied with the liquid crystal substance until a slightly viscous suspension was obtained [30, 31]. The phase thus prepared was pressed between two KBr-plates roughened in advance in one direction had been by means of fine sandpaper (C800 [31]). The moving against each other of the KBr plates is used for promote of the additional orientation of the liquid crystal suspension. The process in our system cannot be described with Couette flow, using the continuum Leslie-Ericksen theory [32], where the orientation of pure liquid crystal is promoted by moving of the plates. The colloidal suspensions are different systems because of their properties, that is the long-range deformation field created by the particles in the liquid crystal, as a result of the director anchoring of the particle surface. In the dipole configuration the particle is accompanied by a topological point defect, whereas in the Saturn-ring configuration the particle is surrounded by a −1/2 disclination ring at the equator [3, 33]. The orientation defects observed near colloidal particles in a nematic liquid crystal have been studied intensively [6, 7, 13, 34–41]. It is well known that when solid particles are introduced into a nematic medium, the nematic molecules prefer to orient at a certain angle on the particle surface, e.g. perpendicularly in so called homeotropic anchoring. It is observed on KBr-plates as well. We postulate that the threshold for these processes would be lowered by a significant amount by first roughening the KBr-plates and then moving the system in a single direction t. In [7] it was has been noted that the anchoring direction of particle surfaces would come into conflict with far field orientation. It is believed that the resulting defects play a critical role in the interactions between the particles and the novel microstructures formed [8, 9, 42, 43]. These assumptions are more important in our case where the suspended particles are far from being ideal spheres. The Frank theory or linear elastic theory based on that the molecule orientation distribution being uniaxial about the director **n** breaks down in such cases [8, 9, 42, 43]. Some of the phenomena discussed remained negligible when we moved the KBr-repeatedly backwards and forwards in a single direction (100 times [31]) with a velocity of 3 μm/s causing orientation of the suspended particles (Scheme 1), which also promotes orientation. Hence roughening the KBr plates in advance is advantageous. Effective orientation of the sample is achieved when the separation between the two KBr-plates, i.e. cell thickness, is 100 μm. Measurements must be carried out within 2 h of preparation of the system

because there is significant breakdown in the degree of orientation after this period (see below).

The polarized measurements are made in the classical manner [15, 17]. Hence the polarized IR-LD spectra recorded were the perpendicular spectrum, (IR$_\perp$, resulting from a 90° angle between the polarized light beam electric vector and the orientation of the sample), the parallel spectrum (IR$_\parallel$) obtained with a co-linear mutual orientation together with a non-polarized spectrum of the partially oriented suspension (Scheme 2).

The procedure for the position (v_i) and integral absorbancy (A_i) determination for each i-peak was carried out by deconvolution and curve-fitting at a 50:50% ratio of Lorentzian to Gaussian peak functions, χ^2 factors within 0.00013–0.00008 (in our case) and 2000 iterations [30, 31]. The means of two treatments were compared by the Student t-test. The experimental IR-spectral patterns were acquired and processed by means of the GRAMS/AI 7.01 IR spectroscopy (Thermo Galactic, USA) and the STATISTICA for Windows 5.0 (StatSoft, Inc., Tulsa, OK, USA) program packages.

Spectroscopic and structural results obtained by our new orientation technique were obtained using the established reducing-difference procedure designated as "stepwise reduction" for polarized IR-spectra interpretation. This method was initially suggested by Thulstrup and Eggers for the interpretation of polarized UV-spectra [16]. The procedure involves consecutive elimination of the spectral bands of a given polarization by subtracting the perpendicular spectrum multiplied by a coefficient from the parallel one. This procedure was extended by Spanget-Larsen [44] and by Korte and Lampen to samples orientated in stretched polyethylene and in nematic solution, respectively. A systematic analysis of this approach and its application to IR-band assignment according to their symmetry appurtenance was developed by Jordanov and co-workers [45, 46]. The method consists of subtraction of the perpendicular spectrum, (IR$_\perp$, resulting from a 90° angle between the polarized light beam electric vector and the orientation of the sample) from the parallel one (IR$_\parallel$) obtained with a co-linear mutual orientation. The recorded *difference* (IR$_\parallel$–IR$_\perp$) spectrum
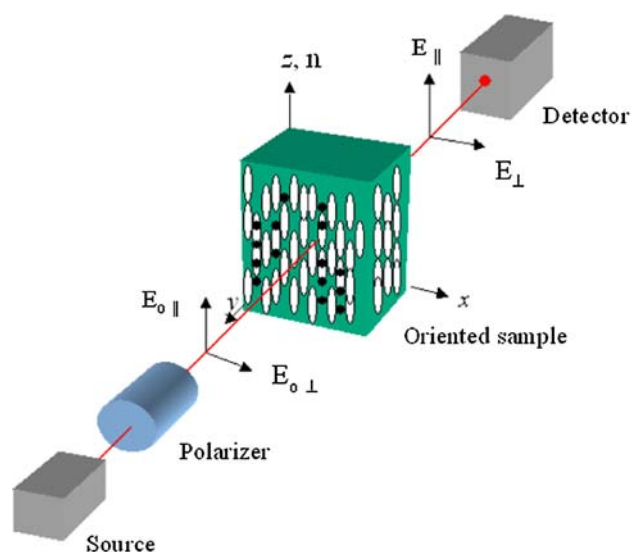

Scheme 2 Optical scheme of an IR-LD experiment

divides the corresponding parallel (A$_\parallel$) and perpendicular (A$_\perp$) integrated absorbencies of each band into positive values originating from transition moments, which form average angles with the orientation direction (**n**) between 0° and 54.7° (magic angle), and negative ones corresponding to transition moments between 54.7° and 90°. In the *reducing-difference procedure*, the perpendicular spectrum multiplied by the parameter **c**, is subtracted from the parallel one and **c** is varied until at least one band or set of bands is eliminated. The simultaneous disappearance of these bands in the *reduced* IR-LD spectrum (IR$_\parallel$–**c**IR$_s$) obtained indicates co-linearity of the corresponding transition moments, thus yielding information regarding the mutual disposition of the molecular fragments.

The lower degree of orientation of the sample makes it impossible to carry out the next IR-LD spectral analysis and apply the reducing-difference procedure. The quantitative approach to answering the question posed lies in calculation of the differences between most intensive and negative bands in the corresponding difference IR-LD spectrum, or $[(A^{v1}_\parallel - A^{v1}_\perp) - (A^{v2}_\parallel - A^{v2}_\perp)]$ for two absorption peaks, corresponding to integral absorbencies in the

Scheme 1 Preparing of the oriented colloidal suspension in nematic liquid crystal
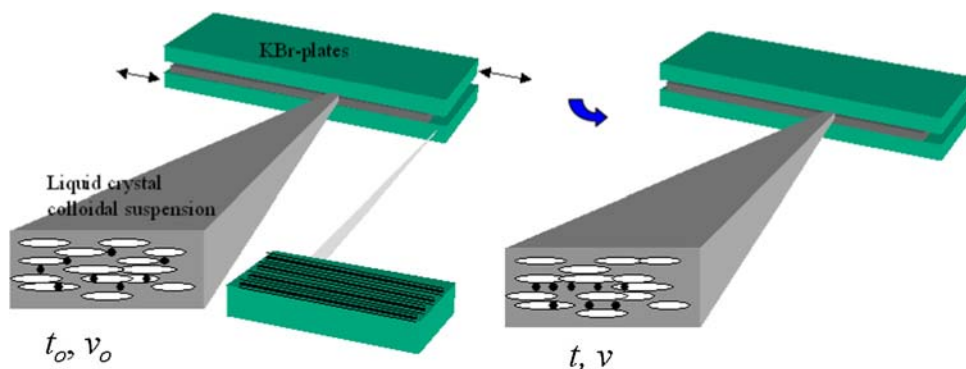
difference spectrum (Fig. 2). The value obtained is designated Δ [31]. The parameter Δ, contains with un evident form the parameter dichroic ratio (R = $A_{\parallel}/A_{\perp}$). However, for obtaining of adequate conclusions both peaks must be belongs to near to perpendicular oriented transition moments, thus securing their different orientation towards the liquid crystal direction n and in corresponding difference spectrum (Fig. 2). For model system DL-isoleucine [31], the peaks at 1501 and 1417 cm^{-1} assigned to the NH$_3$$^+$-symetric bending ($\delta^s_{NH_{3+}}$) and symmetric COO$^-$stretching ($v^s_{COO^-}$) modes are used for this purpose (Fig. 3(2)).

Microcrystalline samples, with a particle size within 0.1–10.0 μm, were squeezed between two glass plates with a spacer sheet between to give an approximately constant sample thickness.

The morphology of the solid samples, of the roughened KBr plates and of the oriented solid particles (colloidal suspension) on the roughened plates was studied by scanning electron microscopy (SEM, JEOL 5510) in a SEI mode.

Synthesis

Polymorphs of 2-{5,5-dimethyl-3-[2-(2,4,6-trimethoxy-phenyl) vinyl] cyclohex-2-enylidene} malononitrile (**Isopho**) were synthesised [47, 48], the 5-amino-2-methoxypyridine ester amide of squaric acid (**154**), using the procedure in [49]. Monoclinic 4′-hydroxyacetanilide or paracetamol (**para**) was purchased from Sigma-Aldrich, while the orthorhombic polymorph, was synthesised [50, 51]. L-Alanyl-L-alanine

(**H-Ala-Ala-OH**), DL-isoleucine (DL-**Isoleu**) and L-phenylala-nyl-L-phenylalanine (**H-Phe-Phe-OH**) were purchased from Bachem Organics. Polymorphs of glycine (**Gly**) α-, β- and γ-Gly were synthesised [52–56], while the hydrochloride salt of glycyl-homotetrapeptide (**H-Gly-Gly-Gly-Gly-OHxHCl**)– [27]. DL-Isoleu polymorph [57] was used. The chemical formula of compounds studied is illustrated in Scheme 3.

Results and discussion

Which model is applicable as explanation of the processes in our colloidal system?

We agree with a critical review by West et al. [41] on the drag on colloidal particles by a moving nematic-isotropic interface, where the total drag on the particle is presented as a sum (Eq. 1):

$$F_{drung} = F_\sigma = F_b = F_s = F_\eta \tag{1}$$

where

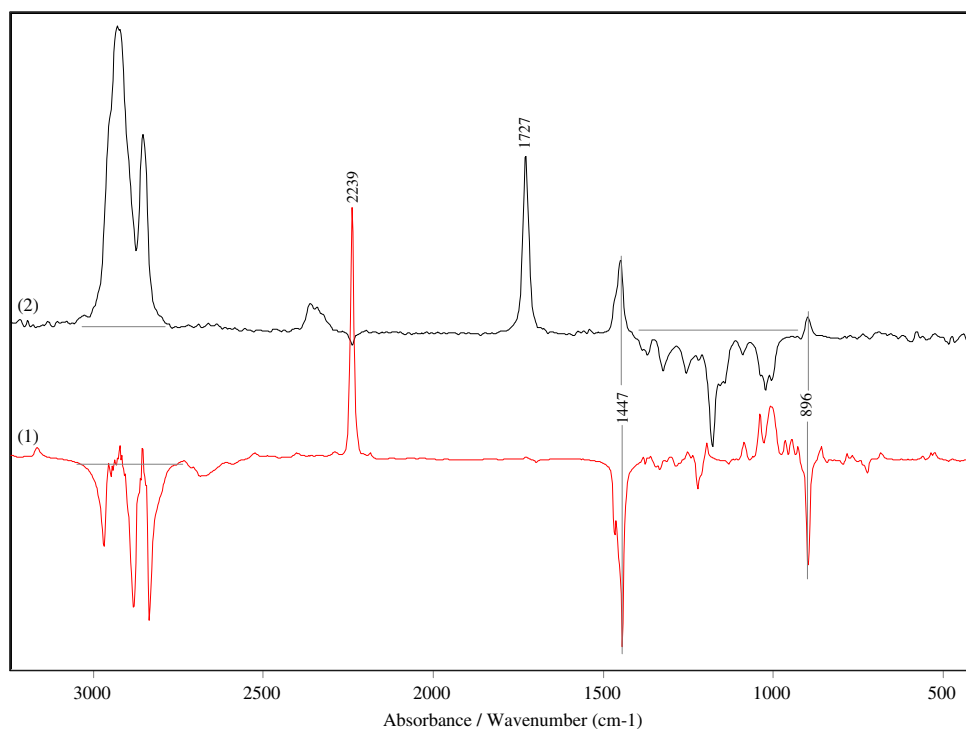$$F_\sigma = 2\pi(\sigma_N - \sigma_I)R[1 - (d/R)^2] \tag{2}$$

$$F_s = WRg_s(d/R) \tag{3}$$

$$F_\eta = -6\pi R\eta v \tag{4}$$

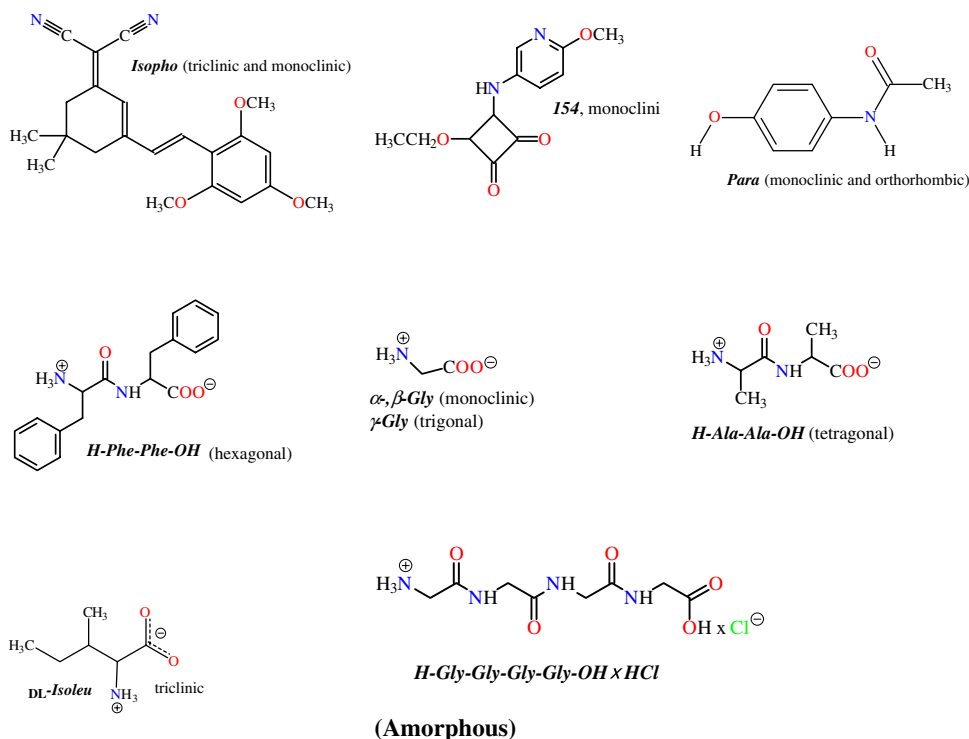$$F_b = W^2R^2/Kg_b(d/R) \quad \text{Or} \tag{5}$$

$$F_b = Kg_b(d/R) \tag{6}$$

The different forces act in the colloidal suspension and several mechanisms affect the total drag force acting on a

Fig. 2 Difference IR-LD spectra of ZLI 1695 (1) and MLC 6815 (2)

Scheme 3 Chemical formula, crystal types and abbreviation used of the compounds studied

Isopho (triclinic and monoclinic)

154, monoclini

Para (monoclinic and orthorhombic)

H-Phe-Phe-OH (hexagonal)

α-, β-Gly (monoclinic)
γ-Gly (trigonal)

H-Ala-Ala-OH (tetragonal)

DL-*Isoleu* triclinic

H-Gly-Gly-Gly-Gly-OH x HCl

(Amorphous)

particle. The surface tension coefficient might differ and an additional pressure (P) caused by the curvature and equation applicable is $P = f(\sigma, R)$ and $\Delta\sigma = \sigma_N - \sigma_I$; R-radius of the particle, σ, surface tension coefficient. This pressure contributes to the total drag force as $F\sigma$ (Eq. 2) with the amplitude growing linearly with the droplet radius, d, distance from the particle center to the interface. $\Delta\sigma$ depends on the surface treatment of the particles and for our system it is unknown and would be difficult to be measure. As in [41] the order of magnitude can be estimated from the change of the surface tension coefficient of each of the organic particle-liquid crystal interfaces and the values of $\Delta\sigma$ lie within the range 10^{-2}–10^{-3} dyn cm^{-2}. The particle creates long-range distortions of the director (**n**) in a nematic phase. In our case to minimize elastic distortion energy, the nematic phase attempts to order particles along axis with direction parallel to (**n**). The elastic forces have two origins: as a result of the director deformations in the bulk nematic phase and as a result of the director being anchored at the particle surface. An estimate of these contributions can be made by dimensional analysis. For the surface contribution, the only combination that has the dimensions of force is WR, where W is the anchoring coefficient. Therefore, the surface contribution to the drag force is proportional to WR, F_s (Eq. 3), where $g_s(x)$ are a dimensionless function of the penetration depth, d/R. One can have two different situations for the bulk contribution. For *weak* anchoring, $WR/K < 1$, the bulk

contribution is proportional to the squared characteristic deviation of the director, $\beta_0 \sim WR/K$. Now W^2R^2/K has the dimension of force, yielding F_b. In the case of strong anchoring, $WR/K \geq 1$, the anchoring does not enter the elastic contribution, and F_b is given with Eqs. 5 and 6, $g_b(x)$ is a dimensionless function. The liquid crystals used here posses typical values of the anchoring energy, $W \sim 10^{-3}$–10^{-4} dyn cm^{-1}. WR/K is <1 for silica particles and WR/K is ~ 1 for polymer particles, respectively. Hence, for silica particles, we have the weak anchorage regime, while polymer particles provide strong anchorage of the director. In our cases we must take both boundaries into account. We also note that the effective radius increases when particles agglomerate and we then have a strong anchorage regime even for small particles. A friction drag contribution, given by the Stokes formula, F_η results in the (Eq. 4) for F_{drag} [41].

Solution of Newton's equations of F_{drag} as a force completes the description of the particle dynamics. It is clear, however, that small heavy particles cannot be moved by the interface (see electron microscopy data). The maximum radius has been estimated from the conservation of linear momentum. To capture a particle of mass m, the interface has to transfer to it a linear momentum mv. If we assume that the particle does not move (or it moves much more slowly than the interface, which is valid for massive particles) then the total linear momentum transferred to the particle is (Eq. 7).

$$mv = \int_{t_1}^{t_2} F_{\text{drag}} dt = \frac{1}{v} \int_{-R}^{R} F_{\text{drag}}(x) dx \qquad (7)$$

If is assumed that the interface touches the particle at time t_1 and leaves it at time t_2, $x = vt$. Substituting F_{drag} is been obtained Eq 8.

$$R_{\max} = \frac{\frac{8}{3}\pi\Delta\sigma + \delta_s W - 6\pi\eta\Delta r}{\frac{4}{3}\pi\rho v^2 - \delta_b W^2/K} \qquad (8)$$

δ_i are geometry parameters, ρ is the density of the particle, and Δr is the final displacement of the particle resulting from the drag force. Several important conclusions can be drawn. First, if the particle is too large, the moving interface is not able to transfer sufficient linear momentum to it. Only particles with $R < R_{\max}$ (v, W, s) will be captured by the interface. Only a slowly moving interface is able to capture the particles. The estimate of this velocity is given by the zero of the denominator of, $v \sim W/(K\rho)^{-1/2} \sim 1$ μm/s. This is of the order of the limiting velocity for the cellular structure we observed in our experiments: if the interface moves more slowly, then stripes appear, otherwise the cellular structure forms.

The main conclusion is that $R_{\max}$ is a function of the material parameters, i.e., can be effectively controlled, for example, by changing the surface treatment of the particles, anchoring energy W. An increase in the anchoring energy leads to an increase of $R_{\max}$. Moreover, sufficiently strong anchoring favors formation of a defect near the particle, contributing to an even higher energetic barrier created by elastic forces. On the other hand, if the particle is captured by the interface, the elastic force scales as R^2, and the opposing viscous drag scales as R. Therefore, there is a minimum radius, $R_{\min}$, starting from which particles will be dragged by the interface. If the particle is dragged by the interface at a constant velocity, then $F_{\text{drag}} = 0$, yielding Eq. 9.

$$R_{\min} = \frac{6\pi\eta\Delta r - 2\pi\Delta\sigma - \gamma_s W}{\gamma_b W^2/K} \qquad (9)$$

where $\gamma_i = gi(0)$ are constants. In order to be moved by the interface, the particles have to be large enough. The elastic forces can only overcome viscous drag when this is the case. Substituting values typical for the liquid crystals employed and using the slowest cooling rate, we obtain $R_{\min} \sim 0.08$–0.15 μm, which agrees well with the degree of orientation of suspended particles obtained experimentally. To explain formation of the striped structure, we note that, in practice, particles aggregate into clusters the particles we are using are 1.0–10 μm in size. As has been noted [41] as an aggregate moves it capture more and more particles, growing in size. The anchoring parameter WR/K also increases and we switch from weak anchorage to the strong anchorage regime. The bulk elastic contribution is then proportional to the elastic constant K and the elastic force is no longer growing as R^2. Therefore, at some R_c, the friction drag overcomes the elastic contribution and the aggregate breaks through the interface. A stripe forms and the particles start to accumulate again. The condition $F_{\text{drag}} = 0$ gives the critical size of the aggregate Eq. 10

$$R_c = \frac{\gamma_b K}{6\pi\eta v - 2\pi\Delta\sigma} \qquad (10)$$

which is about 1 μm for typical experimental values.

The calculation of the critical radius above which the particles cannot be captured by the moving interface; predicts that the critical radius is sensitive to the viscous properties of the host liquid crystal, the value of the anchoring coefficient of the liquid crystal on the particle surface, and the velocity of the moving interface [31]. The critical radius above which the particles cannot be captured by the moving interface has been calculated for the liquid crystals ZLI 1695, MLC 6815 and ZLI 1538, respectively. When the particle size of the suspended particles is less than 0.08 μm reasonable orientation cannot be expected. As has been noted, that the critical radius is sensitive to the viscous properties of the host liquid crystal, the value of the anchoring coefficient of the liquid crystal on the particle surface, and the velocity of the moving interface. In order to understand how the particles are moved by the nematic mesophase transition front we used particles of 13 different organic compounds of different sizes (Scheme 1). The influence of the morphology and of the crystalline particles on the degree of orientation in nematic liquid crystal suspension was studied using a selected set of compounds crystallizing in different polymorph modifications, different space groups and cell settings. The particle size was within the range 0.1–10.0 μm. In all cases the particles were dispersed at concentrations of 5 ± 1% by weight, which had been previously found optimum [31]. The suspension obtained was deposited between two KBr plates that had previously been roughened in one-direction plates. The cell thickness was varied between 50 μm and 150 μm, in order to study the influence of layer of different sizes thickness on the orientation of the sample. The direction of the stripes is parallel to the moving interface, the interface was moving from the left to the right of the cell in the geometry depicted in Scheme 3. The spatial period of the striped structure depended on the time and has been evaluated for of the systems described. These results indicate that the particles are pushed by the moving nematic phase transition front.

What our IR-LD spectroscopic measurements give?

The influence of the nature of orienting medium was studied with the DL-*Isoleu* [57], by varying the liquid

crystal type and the particle size, the velocity of the shearing of the KBr plates and the layer thickness. The experimentally observed data for Δ are collected in Fig. 3(2) and listed in Table S1 and Fig. 4a. The maximal orientation of the suspended particles is obtained at a cell thickness of 100 μm, shearing velocity of 3 μm/s and particle size of 0.5–0.9 μm, using the ZLI 1695 and MLC 6815 as hosts.

Conclusions could be drawn for all of the systems studied under the above stated experimental conditions (Table S2 and Figs. 4a–d and 5a–d). As can be seen from the 3D graphs in Figs. 4a–d and 5a–d, in the example of DL-*Isoleu*, the maximal orientation is obtained in the particle size range within 0.5–0.8 μm, at cell thickness of 100 μm, shearing velocity of 3 μm/s for all of the compounds studied,. It is interesting to note that for DL-Isoleu (Fig. 4a) a reasonable orientation is achieved for particle size of 1 μm, assuming that the orientation depends of the nature of the suspended particles, as has been proposed theoretically (see above and [41]). The role of the crystal type on the degree of orientation was examined studying
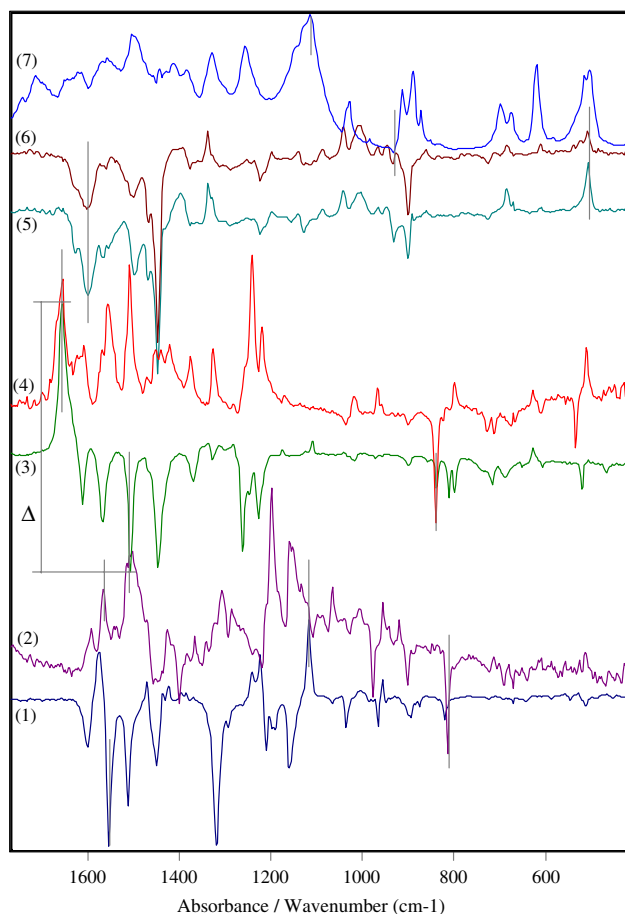

Fig. 3 Difference IR-LD spectra of *Isopho* monoclinic (1) and triclinic (2), *para* monoclinic (3) and orthorhombic (4) polymorphs and *Gly* α- (5), β- (6) and γ- (7) forms

the three compounds with polymorph modifications given in Scheme 3. In all cases the monoclinic and orthorhombic modifications are characterized by a higher Δ, but for the purpose of IR-LD spectroscopy, i.e. IR-band assignment and structural information, the results obtained for all of the crystal types are adequate for the purpose.

The data for both polymorphs of *Isopho*, theΔ data (Fig. 6(1, 2)) are reported in Fig. 4b. The optimum degree of orientation is observed at a shearing velocity of 3 μm, cell thickness of 100 μm and particle size within 0.3–0.5 μm. A reasonable orientation is achieved for aggregates with sizes between 1.0 and 8.0 μm. The triclinic form is characterized by a low degree of orientation of the suspended particles with a Δ difference of 0.30. The above conclusions were also reached for the monoclinic and orthorhombic polymorphs of *para* (Figs. 4c and 6(3, 4)). However, in these systems a reasonable orientation was observed at cell thicknesses of 100 μm. The tendency for a significant orientation of the samples also retained for the α- and β-**Gly** polymorphs, crystallizing with a monoclinic space group (Figs. 4d and 6(5, 6)). From the IR-LD spectroscopic point of view the trigonal polymorph (γ-**Gly**) is oriented (Figs. 4d and 6(7)), independent of the difference of Δ = 0.08 obtained. Like in all of the previous described systems *154* with a monoclinic space group (Figs. 3(1) and 5a) shows an orientation of the suspended particles under the above-mentioned obtained experimental conditions. It is interesting however that in *154*, reasonable values of Δ is obtained at cell thickness of 50 μm, with a Δ difference of 0.02. This means that at the lower concentration of the suspended particles give result capable of interpretation. The result is observed usually in the layered systems, where the orientation of the suspended particles is along the one of the crystallographic axes. In *154* only one is formed by intermolecular interaction of the NH···O=C type with a bond length of 2.955 Å [49] (Scheme 5) and the observation in the difference IR-LD spectrum (Fig. 3(1)) a positive peak about 1800 cm^{-1} for symmetric stretching motion, $v^s_{C=O(Sq)}$ confirms (see experimental part) orientation of the layers along the *b*-axis (Scheme 5).

A reasonable degree of macro orientation of the suspended particles of the tetragonal *H-Ala-Ala-OH* is obtained over the whole in the whole range of particle size range of 0.5–0.8 μm (Figs. 3(4) and 5b) at 100 μm cell thickness. It is interesting to note in this case that the sample orientation is sensitive to the velocity of the shearing of the KBr-plates and the optimal conditions are within 3 ± 0.5 μm/s. As in the previous example hexagonal *H-Phe-Phe-OH* yields maximum orientation at 3 μm/s, 100 μm cell thickness and particles size within the range 0.1–9.0 μm, with a Δ difference between the particle size ranges within 0.02–0.03. An amorphous sample of *H-Gly-Gly-Gly-Gly-OHxHCl* is oriented in significant level at a shearing velocity 3 ± 0.5 μm/s

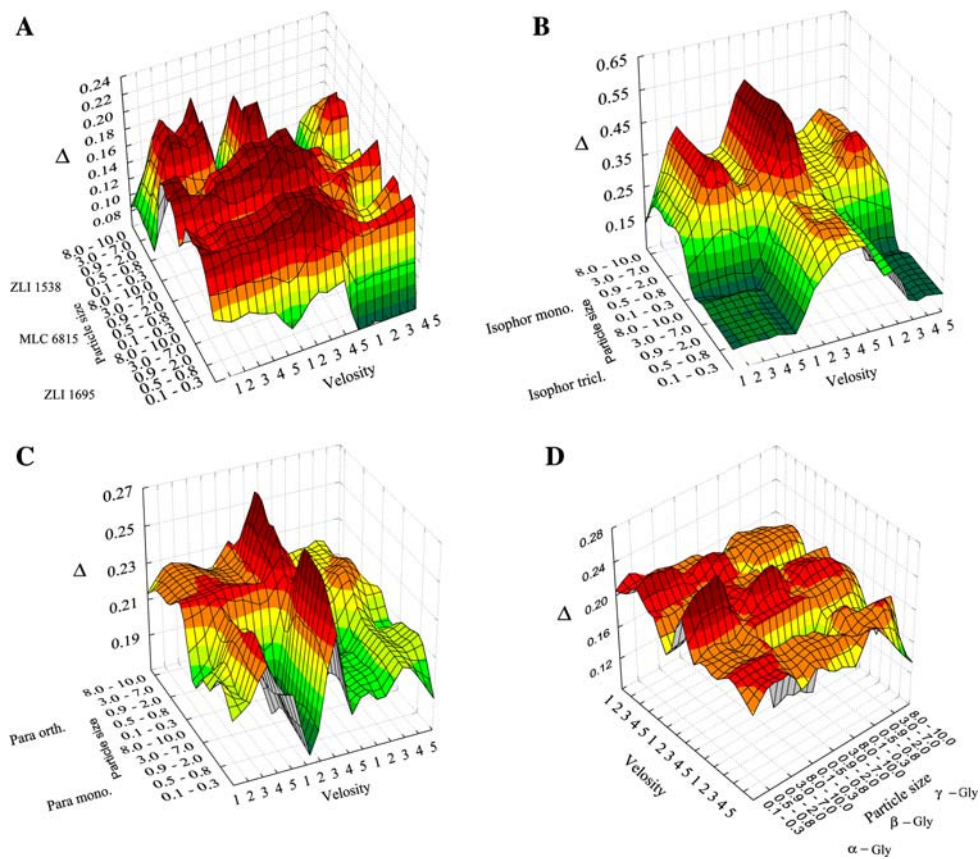**Fig. 4** 3D graph with dependence of the parameter Δ vs. particle size (μm) and velocity of the slippage (μm/s) and layer thickness of the suspension of DL-*Isoleu* in nematic liquid crystal ZLI 1695, MLC 6815 and ZLI 1538 (**a**); polymorphs of ***Isopho*** (**b**), *para* (**c**) and Gly (**d**) in ZLI 1695

Fig. 5 3D graph with dependence of the parameter Δ vs. particle size (μm) and velocity of the slippage (μm/s) and layer thickness of the suspension in nematic liquid crystal ZLI 1695 of ***154*** (**a**), ***H-Ala-Ala-OH*** (**b**), ***H-Phe-Phe-OH*** (**c**) and ***H-Gly-Gly-Gly-Gly-OHxHCl*** (**d**)
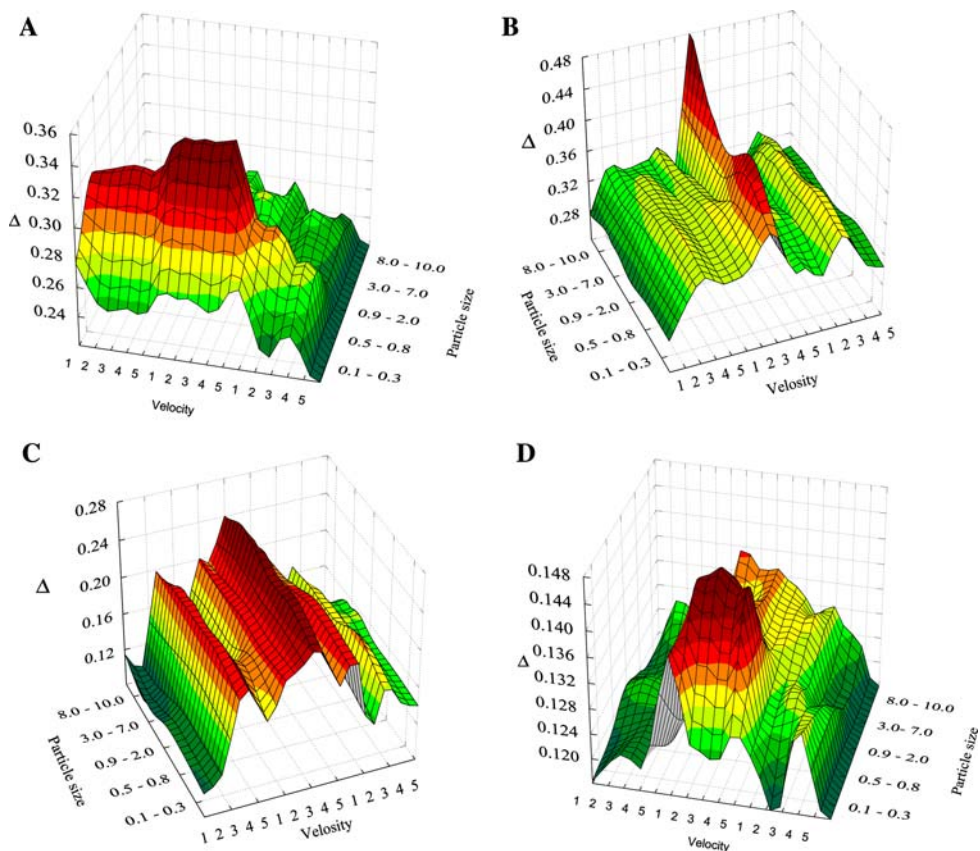
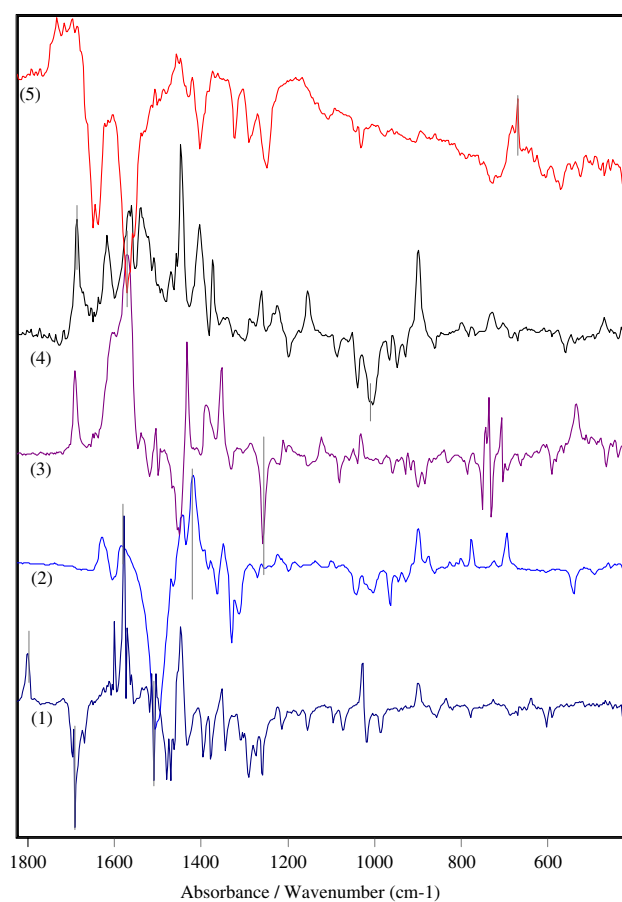**Fig. 6** Difference IR-LD spectra of *154* (1) ᴅʟ-Isoleu (2), PPic (3) alal (4) and GGGG (5)

and particles size within 0.1–0.8 μm range at 100 μm cell thickness (Figs. 3(5) and 5d).

### Accounting for the percentage of the oriented particles in the nematic liquid crystal suspension

A comparison of the degree of orientation of both poly-morphs of Isopho oriented as colloidal suspension in nematic liquid crystal and as polycrystalline sample ori-ented by melting between two KBr-plates, a classical technique for orientation of solids, reveals that that about 15–20% of the particles are oriented in our method. These data correlate well with the electron microscopy observa-tions (Schemes 4 and 5) and can be explained by the fact that the sample contains a wide range of particle dimen-sions (100 nm–10 μm) while the theoretical requirement for maximum orientation in the present study is for parti-cles in the 0.5–0.9 μm ranges. The use of suspended particles of optimum size (within the dimensional range discussed) results in a degree of orientation of 88–91%, depending on the type of compound embedded. As it can be seen in Scheme 4 in some cases, we observe an orien-tation of agglomerates. Independently of this the method is
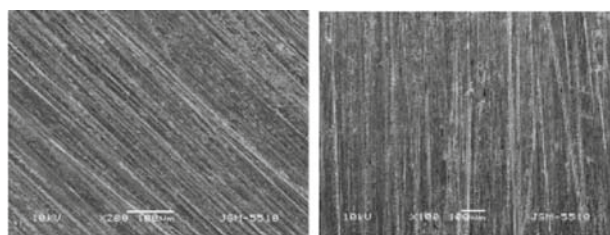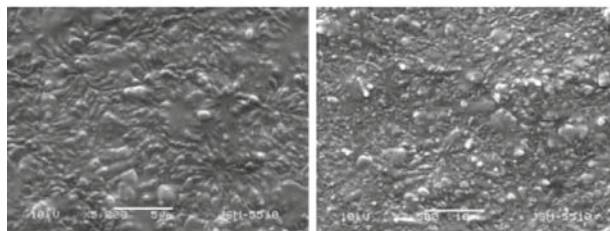

KBr-plates roughened in advance
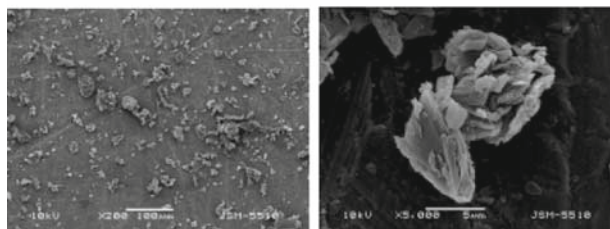
Solid sample and an agglomerate
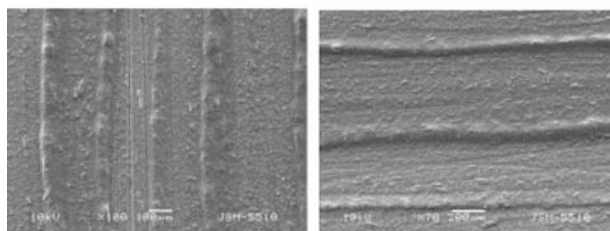
Oriented colloidal suspension on a roughened KBr plate

Dry fragments in the oriented colloidal suspension

Scheme 4 Electron microscopic data

informative since the difference IR-LD spectrum only reveals that embedded compound that is oriented. In the case of non-oriented particles, the $A_{\parallel}$ and $A_{\perp}$ for given v_i is equal and subtracting both spectra at subtracting parameter 1, results in a zero-base line.

How are stable the oriented structures of suspended particles in the nematic liquid crystal medium?

In all cases the prepared samples must be measured in the time interval of 0–120 min. After that depending on the type of the suspended particles we observe a significant increase in the level of disordered particles, accompanied with the formation of star-like structures for example (Scheme 4), resulting in a low values of Δ.

The method of oriented colloid suspension in nematic liquid crystal is applicable for structural elucidation of all

Scheme 5 Crystallographic data for **154** and the direction of the $\nu^{s}_{C=O(Sq)}$ transition moment
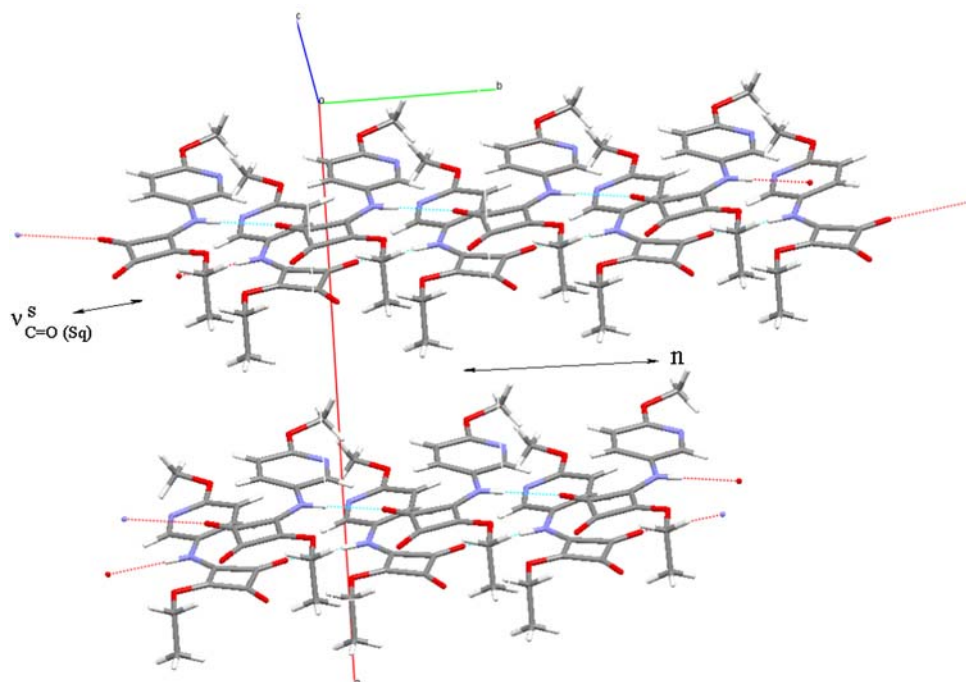
the compounds studied here [24, 27, 31, 58, 59] and the validity of the conclusions reached is confirmed by their established crystallographically determined structures.

An experimental design of the type full factorial design on two levels of variation of the input factors (2^3) was used to estimate the impact of the experimental parameters (size, shearing velocity, thickness) on the analytical signal for each system investigated. The information matrix of the design and the experimental results with assessment of the experimental bias (analytical signal, signal intensity) is reproduced in Table S3. The three input factors X_1, X_2, and X_3 are, respectively size, shearing velocity and thickness. The two levels of variation of the factors normalized as +1 and −1 are as follows: X_1 (0.3–0.1 (−) and 0.9–2.0 (+)), X_2 (2 (−) and 4 (+)) and X_3 (50 (−) and 150 (+)), respectively.

The experimental design makes it possible to construct a polynomial regression model, which represents the impact of the single factors or their combination on the output function. Models for each of the systems considered were constructed and checked for variance homogeneity, regression coefficient significance and model fit. The validity tests revealed that only a few regression coefficients were statistically significant (higher values than the significance number, which estimates the experimental error) and need to taken into account in the data interpretation. Table 1 gives the linear regression coefficients for each system together with the number of significance for each of the models. No mixed coefficients are presented since all of them were statistically insignificant.

The free term of the regression a_0 is a measure for the average signal intensity, the coefficients a_1, a_2, a_3 reflect the impact of the experimental parameters involved.

As seen, maximal signal intensity is registered for the systems **Isopho** monoclinic form, **H-Ala-Ala-OH** (higher than 0.3), followed by **154**, **para** orthorhombic and monoclinic forms, **Gly** systems (between 0.2 and 0.26). Lowest intensity is indicated by the systems **H-Phe-Phe-OH**, **Isopho** triclinic and amorphous **H-Gly-Gly-Gly-Gly-OHxHCl**. (lower than 0.2).

The experimental factor "size" shows significance only for three systems (**H-Phe-Phe-OH**, **154**, and γ-**Gly**) and its impact is always negative. It may be concluded that its role in the signal formation is not substantial except for the system **154** where lower size causes a better output signal.

Four out of eleven insignificant regression coefficients (**Isopho** triclinic, **para** orthorhombic and monoclinic forms, **H-Gly-Gly-Gly-Gly-OHxHCl**) are marked for the second experimental factor (shearing velocity). The effect of a_2 is predominantly negative, which means that a lower shearing velocity offers opportunity for a higher signal.

Only the system **H-Ala-Ala-OH** indicates insignificance with respect to the impact of the input factor "layer thickness" on the output signal. Therefore, this is the most important experimental factor for almost all systems. Its effect is predominantly negative, which means that better signals are obtained for a lower layer thickness.

For illustration of the factor impact the following four plots are given (Scheme 6).

In this study we face a problem, which could also be handled by the use of multivariate statistical approaches.

Table 1 Linear regression coefficients

	a_0	a_1 (size)	a_2 (velocity)	A_3 (thickness)	Significance number
H-Gly-Gly-Gly-Gly-OHxHCl	0.1228	0.00025	−0.00025	0.002	0.0013
154	0.2591	−0.01263	−0.00188	−0.006375	0.0016
Isoph triclinic form	0.1446	0.000625	−0.00088	0.024125	0.002
Isoph monoclinic form	0.3469	0.001375	0.019375	−0.01	0.0024
Para monoclinic form	0.2084	0.000625	−0.00063	−0.005125	0.0013
Para orthorhombic form	0.2249	0.000375	0.000125	−0.004375	0.0018
α-Gly	0.2041	0.000375	−0.00213	−0.002375	0.0007
β-Gly	0.2001	0.001375	0.006375	−0.006875	0.0015
γ-Gly	0.1929	−0.00113	−0.00138	−0.0011375	0.0011
H-Ala-Ala-OH	0.3384	0.001	−0.00763	−0.000625	0.0016
H-Phe-Phe-OH	0.1536	−0.00138	0.021375	−0.008875	0.0011

Scheme 6 Relative intensity level (a_0 impact) for all systems studies (**a**), Effect of the size parameter (a_1 impact) on the output signal for all systems (**b**), Effect of the velocity parameter (a_2 impact) on the output signal for all systems (**c**) and Effect of the thickness parameter (a_3 impact) on the output signal for all systems (**d**)
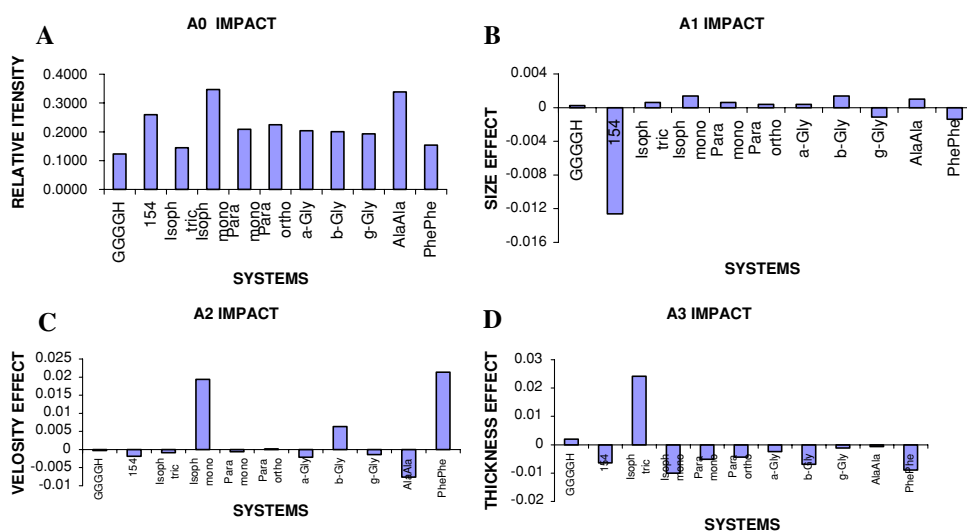
Each of the 11 systems involved was be successfully described by a row of reliable descriptors, e.g. the regression coefficients from the models representing the impact of each experimental parameter on the output signal. When cluster analysis was applied to the results (11 objects each one of them described by four coefficients having their own physical meaning and impact) one should find levels of similarity (or dissimilarity) between the systems studied. As is known (*Ref.*) cluster analysis is a very important classification and projection method, which makes it possible to plot a multidimensional system on a plane and to detect groups of similarity (clusters) on the plot. In our case we applied hierarchical agglomerative clustering of the normalized input data (z-transformation), squared Euclidean distance as a measure of similarity and Ward's method of linkage between the objects (or between the variables).

As can be seen from Figs. 7 and 8. below a high level of similarity is observed between all *Gly* systems and *para* systems. The *H-Ala-Ala-OH* object could be included with the big cluster of *Gly* and *para* systems. This means that all
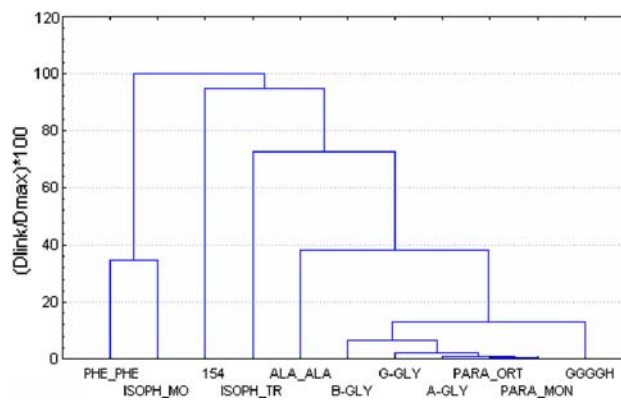
Fig. 7 Dendrogram for 11 objects (systems in consideration)

these experimental systems behave in quite a similar manner with respect to their analytical signal and experimental parameter impacts. A medium level of relative signal intensity and a not very strong impact of the experimental parameters characterize them. In a way these
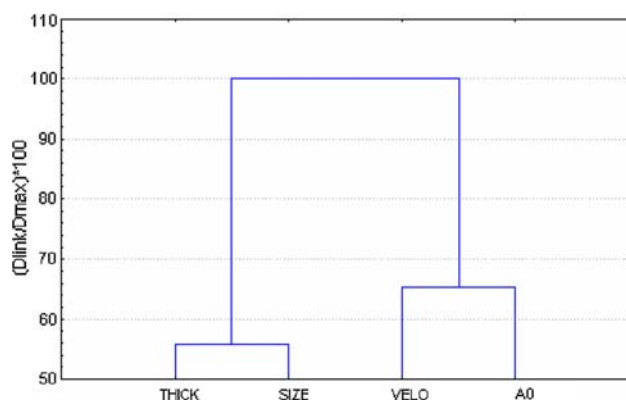
Fig. 8 Dendrogram for clustering of the variables

systems could be easily exchanged with each other in reaching certain signal intensity despite the various experimental conditions. The o *H-Gly-Gly-Gly-Gly-OHxHCl* system also belongs to this cluster.

The systems *H-Phe-Phe-OH* and *Isopho* monoclinic form also form a group of similarity on account of their very strong dependence on the shearing velocity parameter. Although having different relative intensity values, they prove to be similar on the basis of strong a_2 impact (positive influence). The relatively high (although negative) influence of the thickness parameter also plays a role in this case. No other system is influenced so significantly by the simultaneous impacts of the layer thickness and shearing velocity parameters.

The remaining systems *154* and *Isopho* triclinic differ from the other two groups of similarity and occupy the position of outliers rather than belonging to a separate group. They indicate quite different intensities and impacts of the input parameters and should be considered as individual cases with respect to their output signal and response to the experimental conditions.

Since a clustering of the systems in consideration is obtained, it was important to check if the system descriptors (regression coefficients) are correlated in one way or another. The cluster analysis with respect to the variables yielded the dendrogram reproduced in Fig. 8.

Two distinct groups of descriptors are formed. It may be assumed that two major factors are responsible for the linkage between the system descriptors—the first one indicating linkage between relative intensity and velocity (conditional name "dynamic" experimental factor) and the second one (conditional name "static" experimental factor) demonstrating the correlation between size and thickness parameters. Both groups are quite different in their impact on the system's response.

The statistical modeling of the systems has made it possible to understand the role of some important experimental parameters on the analytical signal formation and

this is an important step in the optimization of the analytical procedure using the approach. Moreover, similarities and dissimilarities have been found between the various experimental systems and their statistical descriptors, which is another step towards analytical optimization.

In conclusion, what we are presenting?

A new linearly polarized IR-spectroscopic tool for studying of structure and orientation of *colloidal suspensions*, oriented in nematic liquid crystal. The method could be applied to suspended particles organic compounds, transition metal complexes, inorganic materials and glasses, their structural and IR-spectroscopic elucidation in solid state. Independently of that, the method permits the orientation of particles with sizes within 0.3–0.9 μm, it could also be applied to the study of aggregates (1–2 μm) too, but in very limited cases. The procedure is cheap, rapid and simple with respect to explanation and interpretation, requiring knowledge on IR-characteristics of embedded solids. The great advantages of the method are connected namely the possibility of obtaining of structural and local structural information for amorphous samples and glasses, where the application of the unique structural method as single crystal X-ray diffraction method is impossible. It should also be applicable to polycrystalline samples and to low quality single crystals.

References

1. Soville, D.A., Russel, W.B., Schowaiter, W.R.: Colloidal dispersions. Cambridge University Press, Cambridge (1989)
2. Ruhwandl, A.P., Zukoski, E.M.: Electrorheological fluids as colloidal suspensions. Adv. Collid. Interface Sci. **30**, 153 (1989)
3. Poulin, P., Stark, H., Lubensky, T.C., Weitz, D.A.: Novel colloidal interactions in anisotropic fluids. Science **275**, 1770 (1997)
4. Poulin, P., Frances, N., Mondain-Monval, O.: Suspension of spherical particles in nematic solutions of disks and rods. Phys. Rev. E **59**, 4384 (1999)
5. Borstnik, A., Stark, H., Zumer, S.: Interaction of spherical particles dispersed in a liquid crystal above the nematic-isotropic phase transition. Phys. Rev. E **60**, 4210 (1999)
6. Lev, B.I., Aoki, K.M., Tomchuk, P.M., Yokoyama, H.: Structure formation of colloids in nematic liquid crystals. Condens. Matter Phys. **6**, 169 (2003)
7. Feng J.J., Zhou, Ch.: A mean-field study of defects near colloidal particles in a nematic liquid crystal. J. Colloid Interface Sci. **269**, 72 (2004)
8. Terentjev, E.M.: Disclination loops, standing alone and around solid particles, in nematic liquid crystals. Phys. Rev. E **51**, 1330 (1995)

9. Stark, H.: Numerical investigation of liquid crystal colloids using a continuum description. Phys. Rev. **351**, 387 (2001)

10. Loudet, J-C., Barois, P., Poulin, P.: Colloidal ordering from phase separation in a liquid crystalline continuous phase. Nat. Lond. **407**, 611 (2000)

11. Meeker, S.P., Poon, W.C.K., Crain, J., Terentjev, E.M.: Colloid-liquid-crystal composites: an unusual soft solid. Phys. Rev. **E 61**, R6083 (2000)

12. Nazarenko, V.G., Nych, A.B., Lev, B.I.: Crystal structure in nematic emulsion. Phys. Rev. Lett. **87**, 075504 (2001)

13. Stark, H.: Saturn-ring defects around microspheres suspended in nematic liquid crystals: an analogy between confined geometries and magnetic fields. Phys. Rev. E **66**, 032701 (2002)

14. Ivanova, B.B., Arnaudov, M.G., Bontchev, P.R.: Linear-dichroic infrared spectral analysis of Cu(I)-homocysteine complex. Spectrochim. Acta **60A**, 855 (2004)

15. Michl J., Thulstrup E.W.: Spectroscopy with polarized light. Solute alignment by photoselection, in liquid crystals, polymers, and membranes. VCH Publishers, New York (1986)

16. Thulstrup, E.W., Eggers, J.H.: Moment directions of the electronic transitions of fluoranthene. Chem. Phys. Lett. **1**, 690 (1996)

17. Thulstrup, E.W., Thulstrup, P.W.: Polarization spectroscopic studies of ordered molecules. Acta Chim. Slov. **52**, 371 (2005)

18. Frushour, B.G., Painter, P.C., Koening, J.L.: Vibrational spectra of polypeptides. J. Macromol. Sci. **C15**, 29 (1976)

19. Jasse, B., Koening, J.L.: Orientational measurements in polymers using vibrational spectroscopy. J. Macromol. Sci. **C17**, 61 (1979)

20. Zbinden R.: Infrared spectroscopy of high polymers. Academic Press, New York (1964)

21. Siesler H.W.: Characterization of polymer deformation by vibrational spectroscopy. In: Orientated polymer materials. Chap. 4, St. Fakirov (ed.) Huethling Wepf Verlag Zug. Heidelberg, Oxford CT, USA, (1996)

22. Ivanova, B.B.: Solid state linear dichroic infrared spectral analysis of benzimidazoles and their N1-protonated salts. Spectrochim. Acta **62A**, 58 (2005)

23. Ivanova, B.B., Mayer-Figge, H.: Crystal structure. and solid state IR-LD analysis of a mononuclear Cu(II) complex of 4-aminopzridine. J. Coord. Chem. **58**, 653 (2005)

24. Ivanova, B.B.: Monoclinic and orthorhombic polymorphs of paracetamol—solid state linear dichroic infrared spectral analysis. J. Mol. Struct. **738**, 233 (2005)

25. Bakalska R., Ivanova B.B., Kolev, Ts.: Solid-state IR-LD spectroscopy of codeine, N-norcodeine derivatives. Cent. Eur. J. Chem. **4**, 533 (2006)

26. Ivanova, B.B.: Stereo-structural and IR-spectral characterization of histidine containing dipeptides by means of solid-state IR-LD spectroscopy and ab initio calculations. J. Mol. Struct. **782**, 122 (2006)

27. Ivanova, B.B., Kolev, T., Zareva, S.Y.: Mononuclear Au(III)-complexes with tryptophan-containing dipeptides: Synthesis, spectroscopic and structural elucidation. Biopolymers **82**, 587 (2006)

28. Kolev, T.: Solid-state IR-LD spectroscopic and theoretical analysis. of arginine-containing peptides. Biopolymers **83**, 39 (2006)

29. Kolev, T., Koleva, B., Shivachev, B.: Oriented solids as a colloid suspension in nematic liquid crystal as a new tool for IR-spectroscopic and structural elucidation of inorganic compounds and glasses. Inorg. Chim. Acta (2007, in press)

30. Ivanova, B.B., Tsalev, D.L., Arnaudov, M.G.: Validation of reducing-difference procedure in IR-solid mixtures. Talanta **69**, 822 (2006)

31. Ivanova, B.B., Simeonov, V.D., Arnaudov, M.G., Tsalev, D.L.: Linear-dichroic infrared spectroscopy—validation and experimental design of the new orientation technique of solid samples

32. as suspension in nematic liquid crystal. Spectrochim. Acta **67A**, 66 (2007)

33. Forest, M.G., Hong, Q., Zhou, Z.R.: Compare Couette versus Poiseuille flow. J. Rheol. **48**, 175 (2004)

34. Poulin, P., Raghunathan, V.A., Richetti, P., Roux, D.: Colloidal inclusions in liquid crystals. J. Phys. II **4**, 1557 (1994)

35. Andrienko, D., Tasinkevych, M., Dietrich, S.: Effective pair interactions between colloidal particles at a nematic-isotropic interface. Europhys. Lett. **70**, 95 (2005)

36. West, J.L., Zhang, K., Glushchenko, A., Andrienko, D., Tasinkevych, M., Reznikov, Y.: Colloidal particles at a nematic-isotropic interface: effects of confinement. arXiv:cond-mat/0606169 v1 7 Jun 2006

37. Smalyukh, I.I., Lavrentovich, O.D., Kuzmin, A.N., Kachynski, A.V., Prasad, P.N.: Elasticity-mediated self-organization and colloidal interactions of solid spheres with tangential anchoring in a nematic liquid crystal. arXiv:cond-mat/0508331 v1 13 Aug 2005

38. Andrienko, D., Tasinkevych, M., Patrıcio, P., M.M. Telo da Gama. arXiv:cond-mat/0312203 v1 8 Dec 2003

39. Vollmer, D., Hinze, G., Poon, W.C.K., Cleaver, J., Cates, M.E.: The origin of network formation in colloidliquid crystal composites. J. Phys. Condens. Matter **16**, L227 (2004)

40. Stark, H., Fukuda, J., Yokoyama, H.: Capillary condensation in liquid-crystal colloids. Phys. Rev. Lett. **92**, 205502 (2004)

41. Kalyon, D.M., Yaras, P., Aral, B., Yilmazer, U.: Rheological behavior of concentrated suspensions: a solid rocket fuel stimulant. J. Rheol. **37**, 35 (1993)

42. West, J.L., Glushchenko, A., Liao, G., Reznikov, Y., Andrienko, D., Allen, M.P.: Drag on particles in a nematic suspension by a moving nematic-isotropic interface. Phys. Rev. E **66**, 012702 (2002)

43. Lubensky, T.C., Pettey, D., Currier, N., Stark, H.: Topological defects and interactions in nematic emulsions. Phys. Rev. E **57**, 610 (1998)

44. Stark, H.: Director field configurations around a spherical particle in a nematic liquid crystal. Eur. Phys. J. B **10**, 311 (1999)

45. Spanget-Larsen, J.: Infrared linear-dichroism spectroscopy of 1,8-dihydroxy-9,10-anthraquinone aligned in stretched polyethylene. SPIE **1575**, 404 (1992)

46. Jordanov, B., Nentchovska, R., Schrader, B.: FT-IR linear dichroic solute spectra of nematic solutions as a tool for IR band assignment. J. Mol. Struct. **297**. 401 (1993)

47. Jordanov, B., Schrader, B.: Reduced IR-LD spectra of substances oriented as nematic solutions. J. Mol. Struct. **347**, 389 (1995)

48. Kolev, T., Glavcheva, Z., Yancheva, D., Schuermann, M., Kleb, D.-Chr., Preut, H., Bleckmann, P.: Triclinic form of 2-{5,5-dimethyl-3-[2-(2,4,6-trimethoxyphenyl)vinyl]cyclohex-2-enylidene}malononitrile. Acta Crystallogr. **E57**, o966 (2001)

49. Kolev, T., Glavcheva, Z., Yancheva, D., Schuermann, M., -Chr. Kleb, D., Preut, H., Bleckmann, P.: Monoclinic form of 2-{5,5-dimethyl-3-[2-(2,4,6-trimethoxyphenyl)vinyl]cyclohex-2-enylidene}malononitrile. Acta Crystallogr. **E57**, o964 (2001)

50. Kolev, T., Koleva, B.B., Spassov, T., Cherneva, E., Spiteller, M., Mayer-Figge, H., Sheldrick, W.S.: Synthesis, spectroscopic, thermal and structural elucidation of 5-amino-2-methoxypyridine ester amide of squaric acid ethyl ester: a new material with an infinite pseudo-layered structure and manifested NLO application. J. Mol. Struct. (2007, in press)

51. Haisa, M., Kashino, S., Maeda, H.: The orthorhombic form of p-hydroxyacetanilide. Acta Crystallogr. **30B**, 2510 (1974)

52. Nichols, G., Frampton, C.S.: Physicochemical characterization of the orthorhombic polymorph of paracetamol crystallized from solution. J. Pharm. Sci. **87**, 684 (1998)

53. Marsh, R.E.: A refinement of the crystal structure of glycine. Acta Crystallogr. **11**, 654 (1958)

53. Legros, J.-P., Kvick, A.: Deformation electron density of α-glycine at 120 K. Acta Crystallogr. **36B**, 3052 (1980)
54. Shimon, L.J.W., Lahav, M., Leiserowitz, L.: Stereoselective etchants for molecular crystals. Resolution of enantiomorphs and assignment of absolute structure of chiral molecules and polar crystals. New J. Chem. **10**, 723 (1986)
55. Langan, P., Mason, S.A., Myles, D., Schoenborn, B.P.: Structural characterization of crystals of α-glycine during anomalous electrical behaviour. Acta Crystallogr. **58B**, 728 (2002)
56. Boldyreva, E.V., Drebushchak, T.N., Shutova, E.S.: Structural distortion of the α, β, and γ polymorphs of glycine on cooling. Z. Kristallogr. **218**, 366 (2003)
57. Benedetti, E., Pedone, C., Sirigu, A.: The crystal structure of DL-isoleucine and structural relations between racemic and optically active pairs in some amino acids. Acta Crystallogr. **29B**, 730 (1973)
58. Ivanova, B.B.: Solid state linear-dichroic infrared spectral analysis of dipeptide L-Phe-L-Phe and its mononuclear Au(III)-complex. J. Coord. Chem. **58**(7) 587 (2005)
59. Ivanova, B.B.: Solid state linear-dichroic infrared (IR-LD) spectral characterization of α- and β-polymorphs of glycine. Cent. Eur. J. Chem. **4**, 111 (2006)